The Origin of The EUV Emission in Her X-1

D. A. Leahy
Dept. of Physics, University of Calgary, University of Calgary, Calgary, Alberta, Canada
T2N 1N4

and

H. Marshall
M.I.T., Cambridge, MA 02139

ABSTRACT

Her X-1 exhibits a strong orbital modulation of its EUV flux with a large decrease around time of eclipse of the neutron star, and a significant dip which appears at different orbital phases at different 35-day phases. We consider observations of Her X-1 in the EUVE by the Extreme Ultraviolet Explorer (EUVE), which includes data from 1995 near the end of the Short High state, and date from 1997 at the start of the Short High state. The observed EUV lightcurve has bright and faint phases. The bright phase can be explained as the low energy tail of the soft x-ray pulse. The faint phase emission has been modeled to understand its origin. We find: the x-ray heated surface of HZ Her is too cool to produce enough emission; the accretion disk does not explain the orbital modulation; however, reflection of x-rays off of HZ Her can produce the observed lightcurve with orbital eclipses. The dip can be explained by shadowing of the companion by the accretion disk. We discuss the constraints on the accretion disk geometry derived from the observed shadowing.

1. Analysis of the 1995 EUV Observations

Hercules X-1 was observed with the Extreme Ultraviolet Explorer (EUVE) on June 24-28, 1995 (TJD = JD-2440000 = 9893.0 - 9897.1). Using the 35 day ephemeris from BATSE and XTE/ASM observations (Scott, private communication) for phase 0 of 34.85N + MJD50077.0, the 35 day phase of the EUVE observations is 0.71 - 0.82. Phase 0 is defined as turn on of the Main High state. Fig. 1 shows the EUVE DS count rate for these data and Fig. 2 shows the lightcurve folded at the binary period, with some curves described below. There is a large dip near binary phase 0.5 where the neutron star is in front of the companion.

To determine the origin of the EUVE emission some modelling calculations were carried out (this discussion is similar to that in Leahy & Marshall 1999). The orbital parameters from x-ray timing analysis (Deeter et al. 1991) were used. Additional assumptions were needed for the orbit to calculate light curves: orbital inclination of 85^o, a K_{opt} value of 100 km/s (Reynolds et al. 1997), and a mass ratio of 0.592 (Leahy & Scott 1998). The distance of Her X-1 was assumed to be 6.6 kpc.

1.1. X-ray Heating of HZ Her

Emission from the x-ray heated face of the optical companion HZ Her was calculated as follows. The unheated temperature of the companion was taken to be 8100K. The companion was approximated by a grid of flat surfaces with 19 elements in latitude and 38 elements in longitude. The surface elements were located on the Roche critical surface (and with surface normals perpendicular to this surface), since we assumed that HZ Her is Roche-lobe filling. The incident x-ray flux on the surface of the companion, HZ Her, was assumed to be locally absorbed and re-radiated with a blackbody spectrum. The neutron star x-ray luminosity was taken as $2 \times 10^{37} erg\ s^{-1}$ radiated isotropically. The large dip near binary phase 0.5 can be modelled by occultation of the companion by the accretion disk.

Lightcurves were constructed by rotating the binary system and calculating the EUV emission for each orientation. We include the reduction in model intensity due to interstellar absorption and the EUVE DS response curve. The main result of the above calculation is that the model count rate is smaller than the observed count rate by a large factor. The conclusion is that this x-ray heating model fails to explain the data.

1.2. Accretion Disk EUV Emission

The accretion disk has two sources of EUV emission: the x-ray heated surface (illuminated by the pulsar); and the emission from self-heating by viscous dissipation in the disk.

First we consider emission from the x-ray heated surface of the disk. The size and shape of the heated region which is visible to the observer depends in detail on the geometry of the twisted and tilted disk. To estimate the emission from the disk, we approximate the heated surface by a blackbody of circular shape (normal to the line-of-sight), with radius R and temperature T, and then require the model count rate (including interstellar absorption and the EUVE DS spectral response) to be 0.03 c/s. This gives a single constraint relating

R and T. E.g. for a column density of $5 \times 10^{19} cm^{-2}$, $T = 10^5 K$ gives $R = 5.9 \times 10^9 cm$, and $T = 10^6 K$ gives $R = 8.5 \times 10^6 cm$.

Next we consider the emission from a standard α-disk, with the temperature-radius relation: $T = 1.5 \times 10^5 (R/10^9 cm)^{-0.6} K$. We include interstellar absorption and then fold an approximation to the spectrum with the EUVE DS spectral response to determine a model EUVE DS count rate. For a face-on, unobscured disk face, and a column density of $5 \times 10^{19} cm^{-2}$, the model count rate is several times the observed count rate. The model emission comes from the part of the disk within $10^9 cm$ of the center, where the disk temperature is more than $1.5 \times 10^5 K$. If one includes the effect of high inclination of Her X-1, and that the disk is twisted and tilted, the model count rate will be reduced by a factor which is sensitive to details of the geometry, so is consistent with the observed DS count rate.

The disk as source of the EUV emission has the following difficulty. There is no easy way for the disk models to produce the observed strong orbital modulation.

1.3. Reflection of X-rays from HZ Her

Another source of EUV emission is the long wavelength part of the spectrum of scattered x-rays from the system. The x-ray spectrum of Her X-1 below a few hundred eV is dominated by the blackbody component (McCray et al. 1982, Vrtilek et al. 1994, Mavromatakis 1993, Dal Fiume et al. 1998). We take the reflecting layer as a thin layer located at the Roche critical surface, and assume that a fraction, R, of the incident x-ray flux is scattered isotropically. R is taken as independent of energy, so that the spectrum of the scattered radiation is the same as that of the incident radiation. The resulting light curve is shown in Fig. 2 by the solid line for a value of R=0.5. The light curve for R=0.25 is shown by the dashed line. The observed data points folded at the orbital period are also shown. The large dip near orbital phase 0.5 is not produced by the model, but the rise near orbital phase 0.3 and decrease near orbital phase 0.7 are in good agreement with the data. The R=0.25 model fits the average level of emission better, but does not match the shape of the observed light curve well. Thus we adopt the R=0.5 model for further discussion.

1.4. Origin of the Dips

Next we discuss the large dips near orbital phase 0.5. The observed dips at TJD9894.2 and TJD9895.8 have intensity reductions of 73% and 56%, resp. First we describe a simple

model to fit the observed light curves including the large dips. The light curve for reflected intensity, with $\eta = 0.5$, was calculated as above, then multiplied by a shadowing function. The shadowing function was of the form: $(1 - \alpha\ exp(-(\phi - \phi_o)^2/2\sigma^2))$, with ϕ is orbital phase. The parameters α, ϕ_o and σ were allowed to have different values for the two observed orbits, and were varied to achieve a good fit to the data. Since there was no improvement in allowing the two values of σ to be different, they were set to be the same, giving $\sigma = 30^o$. The resulting model light curve is shown in Fig. 3 by the solid line, with the data points plotted as the circles. The resulting parameter values are: $\alpha = 0.85$ and $\phi_o = 189^o$ for the first orbit; $\alpha = 0.8$ and $\phi_o = 178^o$ for the second orbit.

Next we discuss the physical origin of the dips. One can achieve a reduction in flux by blocking the line-of-sight to HZ Her by the accretion disk. Calculation shows that the reflected x-rays come fairly uniformly from the whole face of HZ Her, so one needs an object nearly the same size as HZ Her to achieve the observed large flux reductions. (In contrast, for the x-ray heating model, the EUV emission was highly concentrated near the L1 point so the accretion disk could easily block the emission). The reduction in reflected flux for the case of a spherical occulting surface of radius R (centered on HZ Her) is calculated to give an estimate of the required size of an occulter. The results are that the reduction in flux is a smooth function of R/R_{HZHer}. Sample values of the flux reduction are: 10% at $R/R_{HZHer} = 0.26$, 50% at $R/R_{HZHer} = 0.61$, 80% at $R/R_{HZHer} = 0.83$.

The largest object available for occultation in the system is the accretion disk. The radius of the outer edge of the disk is somewhat less than that of the Roche lobe of Her X-1, which is at $2 \times 10^{11} cm$, (calculated using the binary parameters of Leahy & Scott 1998). Schandl & Meyer 1994 gives a better limit on the accretion disk radius, based on the observed orbital period change, of $1.7 \times 10^{11} cm$. The disk model of Schandl & Meyer 1994 has an outer edge inclination of $\sim 7^o$, which results in a flux reduction of 13% for the most favorable disk orientation, assuming a system inclination of 85^o. Thus occultation is not capable of explaining the dips near orbital phase 0.5.

The alternative explanation is that HZ Her is shadowed from the x-ray source by the accretion disk. The accretion disk then only needs to subtend a significant angular extent viewed from the neutron star. For the geometry of Her X-1, the angular radius of HZ Her viewed from the neutron star is 25^o. Significant shadowing of this can occur with a twisted tilted accretion disk. An example of a calculated shadow is given by Figure 5 of Still et al. 1997, which shows ~25% of the front side of HZ Her shadowed for the particular disk parameters they have chosen. Schandl & Meyer 1994 give a sketch of a similar disk (their Fig.13), and a depiction of the shadow the disk casts on the sky as viewed from the neutron star (their Fig. 12).

The amount of shadowing can be calculated from existing disk models. The result depends on the disk tilt and on the disk twist. The maximum tilt is $\sim 10^o$ in the model of Schandl & Meyer 1994, but higher in other models (e.g. Scott 1993 has a maximum tilt of 30^o). Models with a maximum disk tilt of 10^o cannot give a flux reduction, even at most favorable orientation, larger than $\sim 30\%$. The larger flux reduction is associated with models with larger twist. A flux reduction of 100% is possible for maximum tilt greater than 25^o, for which case the vertical angular extent of the accretion disk is larger than that of HZ Her. The general conclusion is that shadowing can account for the large dips near orbital phase 0.5. However, the observed strength of the dips, as large as ~60-70%, implies that the maximum disk tilt should be larger than $\sim 20^o$.

Further evidence that the dips are due to accretion disk shadowing comes from the timing of the dips. The disk in Her X-1 precesses counter to the orbit over a 35 day period, so the disk shadow moves to earlier orbital phase by 18^o (or 0.05 in orbital phase) during a single 1.7 day orbit. Equivalently, the shadow has a 1.62 day period. Compare this to the observed dips. The separation between the two minimum intensity points (at JD-2440000 of 9894.22 and 9895.86 in Figure 1) is 1.64 day, with an uncertainty of $\sim$ 0.2 day. (A different way of measuring the same offset is by use of the Gaussian shadow model. It yielded an orbital phase difference between the shadows for the two orbits of 11^o.) Thus the observed dips in the light curve are consistent with an origin in the precessing shadow of the accretion disk, but not consistent with a constant period of 1.7 day.

Next we discuss what shadowing is expected from standard disk models as a function of 35 day phase, and in particular, at the 35 day phase of the observations here. The timing (i.e. orbital phase) of the accretion disk shadow can be predicted from the 35 day phase since they both depend on the orientation of the accretion disk with respect to the observer. The Main High state peaks near 35 day phase 0.12 (Scott & Leahy 1999) so the observer experiences minimum accretion disk blockage at this time. So the shadow on HZ Her should be minimum at orbital phase 0 (when HZ Her experiences the shadow closest to the direction of the observer) closest to 35 day phase 0.12. However we observe the shadow near orbital phase 0.5. To get the shadow at orbital phase 0.5 we just need to rotate the disk by 180^o, i.e. change 35 day phase by 0.5. Thus the shadow on HZ Her, at orbital phase 0.5, is minimum at 35 day phase 0.62.

The 35-day phase of maximum of disk shadow to the observer depends on the details of the disk model. Tilted-twisted disk models have rings at each radius which cross the binary plane twice over 360^o in azimuth, with an assumed symmetry that has crossings (and maximum excursions from the binary plane) separated by 180^o. This results in maximum shadow at 35 day phases ϕ and $\phi + 0.5$. In the model of Schandl & Meyer 1994, the

maximum shadow follows minimum shadow by 0.23 in 35 day phase (compared to 0.22 for the model of Scott 1993). Thus the shadow should peak at orbital phase 0.5 in this model at 35-day phase 0.85.

From the orbital phases of the two observed dips we estimate the time that the shadow maximum occurs at orbital phase 0.5. This yields a time of JD-2440000 = 9895 or 35 day phase 0.77, which is different from the above prediction of 0.85. The difference could occur for two reasons: 1. The disk twist and tilt are significantly different than in existing disk models, so that maximum follows minimum shadow by only 0.15 in 35-day phase (55^o in azimuth). 2. The minimum obscuration to the observer at 35 day phase 0.12 is offset from the minimum shadowing of HZ Her at orbital phase 0. The latter is hard to achieve, because the observer's inclination to the binary plane is only $\sim 5^o$ (Leahy & Scott 1998). Thus we have evidence here for altered disk parameters which result in a smaller separation of maximum after minimum shadow.

Twisted-tilted disk models with the symmetry described above result in a shadow on HZ Her which repeats twice over the 35 day cycle (except for an inversion about the binary plane). Thus a prediction is that at orbital phase 0.5 and 35-day phase 0.12 the shadowing should be a minimum also. However the EUVE observations of Vrtilek et al. 1994 at this phase show much brighter EUV emission which is pulsed and comes directly from the region of the pulsar. So the much fainter reflected emission off of HZ Her cannot be observed at this phase.

The three narrow dips at JD-2440000 of 9894.54, 9895.53, and 9896.19 are interesting. More observations will be needed to verify their existence. However, if they are verified, they imply a moving structure (with respect to the disk) near the neutron star is causing the shadow. The reason is that a significant (large angular extent) region of HZ Her must be shadowed, but the shadow must move rapidly compared to orbital period for the dip to be of short duration compared to the orbital period. Since two of the narrow dips recur at the same period and orbital phase as pre-eclipse dips, this structure may be the same structure that causes the pre-eclipse dips.

2. Analysis of the 1997 EUV Observations

Fig. 4 shows the EUVE DS lightcurve of Her X-1 at the beginning of short high state on July 25-29, 1997. There is a sharp rise in the EUV flux (by a factor of ~ 10) at TJD 10657. This occurs at 35 day phase 0.57 (using epoch TJD7642.7 and $P_{35} = 34.82d$), consistent with the turn-on phase determined using x-ray observations. Fig. 5 shows an

expanded version to show the flux prior to turn-on more clearly. Fig. 6 shows the light curve as a function of orbital phase.

The EUVE DS flux drops to zero during the predicted time of eclipses. The orbital phase dependence for the orbit before turn-on is similar to that observed in 1995 at the end of short high, but without the large dip near orbital phase 0.5. The peak intensity approximately a factor 2 higher in 1997. This is just what is expected due to the reduced shadowing of HZ Her by the accretion disk: see the model curve in Fig. 2. From disk precession alone, we expect the maximum shadow at the center of HZ Her to shift by 0.2 in orbital phase between turn-on and end of short high. For maximum shadow at orbital phase 0.55 at end of short high (from the 1995 observation), maximum shadow is expected at phase 0.75 at turn-on. There is no obvious shadow maximum at this phase in Fig. 5. The dip at orbital phase 0.85 may be due to the shadow. If so then one needs to explain why the accretion disk shadow has shifted by 0.1 in orbital phase between 1995 and 1997. This may also be caused by a change in the geometry of the disk over the same period.

The bright emission after TJD10657 is as bright as the emission seen previously in the main high state (Vrtilek et al. 1994). The bright emission shows sharp dips at different orbital phases. The dips may be due to the accretion stream. This moves in synchronism with the binary rather than at the 35 day period up until the point where it impacts the disk. It could also be due to the splash at the impact point which is periodic at the binary period but has a complicated path over the disk surface which depends in detail on the disk tilt and twist. Finally we note that the bright emission appears to be blocked from the observer's line-of-sight after orbital phase 0.72. Feasible explanations are blockage of the line-of-sight by the accretion stream or disk impact point splash region. We note that the splash region subtends a much larger angle at the neutron star than the stream so is a better candidate for the extended blockage after orbital phase 0.72. It would be highly desirable to obtain further observations, such as for later orbits in the short high, to test the origin of the dips.

2.1. Pulsations in the 1997 data

We have searched for EUV pulsations by epoch folding and have detected them at high significance. For the first orbit after turn-on (JD2450656.993-2450657.676), the reduced χ^2 vs. period (solid line) and the likelihood vs. period (dashed line) are shown in Fig. 7. The best period is 1.237735 s, with a 9% modulation. For the second orbit after turn-on (JD2450658.654-2450658.885), the reduced χ^2 vs. period (solid line) and the likelihood vs. period (dashed line) are shown in Fig. 8. The best period is 1.237750

s, with a 16% modulation. These periods are consistent with the BATSE pulse monitor measurements for the two Main High states flanking the 1997 EUVE observation. I.e. for epoch JD2450639.47, the pulse period is 1.237730 s, and for epoch JD2450675.31, the pulse period is 1.237731 s.

The pulsations verify that the emission is coming from a region very near the pulsar. Thus they are like the soft x-ray pulsations, which may be reprocessed emission at the inner edge of the accretion disk (e.g. McCray et al. 1982), or alternately, may be directly from high in the accretion column (e.g. Scott 1993).

2.2. The 1997 EUVE SWS Spectrum

Figure 9 shows the EUVE SW spectrometer spectrum of the 1997 data divided into two sections: the bright phase (after TJD10657) and the faint phase (before TJD10657). The faint phase spectrum is too faint to be of much use. The bright phase spectrum is currently being analysed. Figures 10 and 11 present two spectral fits which are preliminary results. Figure 10 assumes $N_H = 0$ and Figure 11 assumes $N_H = 5 \times 10^{19} cm^{-2}$. The results of the two fits are very different, showing how important the N_H value is in modelling the spectrum. Both fits require a power law plus blackbody and have neither a single blackbody or two blackbodies producing adequate fits to the data. However, more work with variable N_H is needed to obtain definite conclusions from the spectrum.

REFERENCES

Dal Fiume, D., et al. 1998, A&A, 329, L41

Deeter,J., Boynton,P., Miyamoto,S., Kitamoto,S., Nagase,F., Kawai,N. 1991, ApJ, 383, 324

Leahy, D.A. 1995, ApJ, 450, 339

Leahy, D., Scott D., 1998, ApJ, 503. L63

Leahy, D., Marshall, H. 1999, ApJ, to appear in Vol. 521.

Malina, R. et al. 1993, AJ, 107, 751

Mavromatakis, F. 1993, A&A, 273,147

McCray et al. 1982 ApJ 262, 301

Reynolds,A., Quaintrell,H., Still,M., Roche,P., Chakrabarty,D., Levine,S. 1997, MNRAS, 288, 43

Rochester,G., Barnes,J., Sidher,S., Sumner,T., Bewick,A., Corrigan,R., Quenby,J. 1994 A&A, 283, 884

Schandl, S., & Meyer, F. 1994, A&A, 289, 149

Scott D. M., 1993, PhD Thesis, University of Washington

Scott D., Leahy, D. 1999, to appear in ApJ vol. 510

Still, M., Quaintrell, H., Roche, P., Reynolds, A., 1997, MNRAS, 292, 52

Vrtilek, S., et al. 1994, ApJ, 436, L9

Fig. 1.— Observed EUVE DS lightcurve of Her X-1 (with $\pm 1\sigma$ error bars) at the end of the short high state on June 24-28, 1995 (TJD = JD-2440000 = 9893.0 - 9897.1). Note the strong orbital modulation of the flux. Broad dips are seen at TJD 9894.2 and 9895.9. In addition there are three narrow dips detected in the EUV lightcurve: at TJD 9894.54, 9895.53, and 9896.19. The orbital phases of these dips is 0.707, 0.301 and 0.684. The first and third dips are pre-eclipse dips and show a separation of 1.62 d, The second dip is likely an anomalous dip.

Fig. 2.— The EUVE DS lightcurve folded at the orbital period. Also shown is the X-ray reflection model lightcurve: for R=0.5 (solid line) and for R=0.25 (dashed line).

Fig. 3.— X-ray reflection lightcurve (solid line) for η=0.5 with the Gaussian shadow model (see text). The EUVE DS data points are shown by the small circles.

Fig. 4.— Observed EUVE DS lightcurve of Her X-1 (with $\pm 1\sigma$ error bars) at the beginning of short high state on July 25-29, 1997 (TJD = JD-2440000 = 10654.7 - 10659.0). Note the sharp turn on in flux as Her X-1 enters the short high state from the low state.

Fig. 5.— Observed EUVE DS lightcurve of Her X-1 (with $\pm 1\sigma$ error bars), but with expanded scale to show more clearly the flux prior to turn-on.

Fig. 6.— Observed EUVE DS lightcurve of Her X-1 (with $\pm 1\sigma$ error bars) at the beginning of short high state on July 25-29, 1997, plotted vs orbital phase.

Fig. 7.— χ^2 vs. period (solid line) and the likelihood vs. period (dashed line) for the first orbit after turn-on.

Fig. 8.— χ^2 vs. period (solid line) and the likelihood vs. period (dashed line) for the second orbit after turn-on.

Fig. 9.— Observed EUVE SW spectrum of Her X-1 during the bright phase (after TJD10657) and during the faint phase (before TJD10657).

Fig. 10.— Bright-phase spectrum of Her X-1 (solid lines are $\pm 1\sigma$ limits) in $ph\ cm^{-2}s^{-1}A^{-1}$ calculated using the EUVE SW response and $N_H = 0$. Blackbody with $T = 90000K$ and radius of $0.006a_x sin(i)$ (dash line); blackbody with $T = 10^7K$ and radius of $7 \times 10^{-6}a_x sin(i)$ (dot line); powerlaw with $\alpha = -6.5$ and normalization at $100A$ of $2 \times 10^{-4}ph\ cm^{-2}s^{-1}A^{-1}$ (dot-dash line).

Fig. 11.— Bright-phase spectrum of Her X-1 (solid lines are $\pm 1\sigma$ limits) calculated using the EUVE SW response and $N_H = 5 \times 10^{19}cm^{-2}$. Blackbody with $T = 90000K$ and radius

of $0.3a_x sin(i)$ (dot line); blackbody with $T = 50000K$ and radius of $7.0a_x sin(i)$ (dash line); powerlaw with $\alpha = 0$ and normalization at $100A$ of $2 \times 10^{-11} ph\ cm^{-2} s^{-1} A^{-1}$ (dot-dash line). The spectra here are in units of $ph\ cm^{-2} s^{-1} A^{-1}$ and have been multiplied by $(100A/\lambda)^4$ to better show the short *lambda* end of the plot.

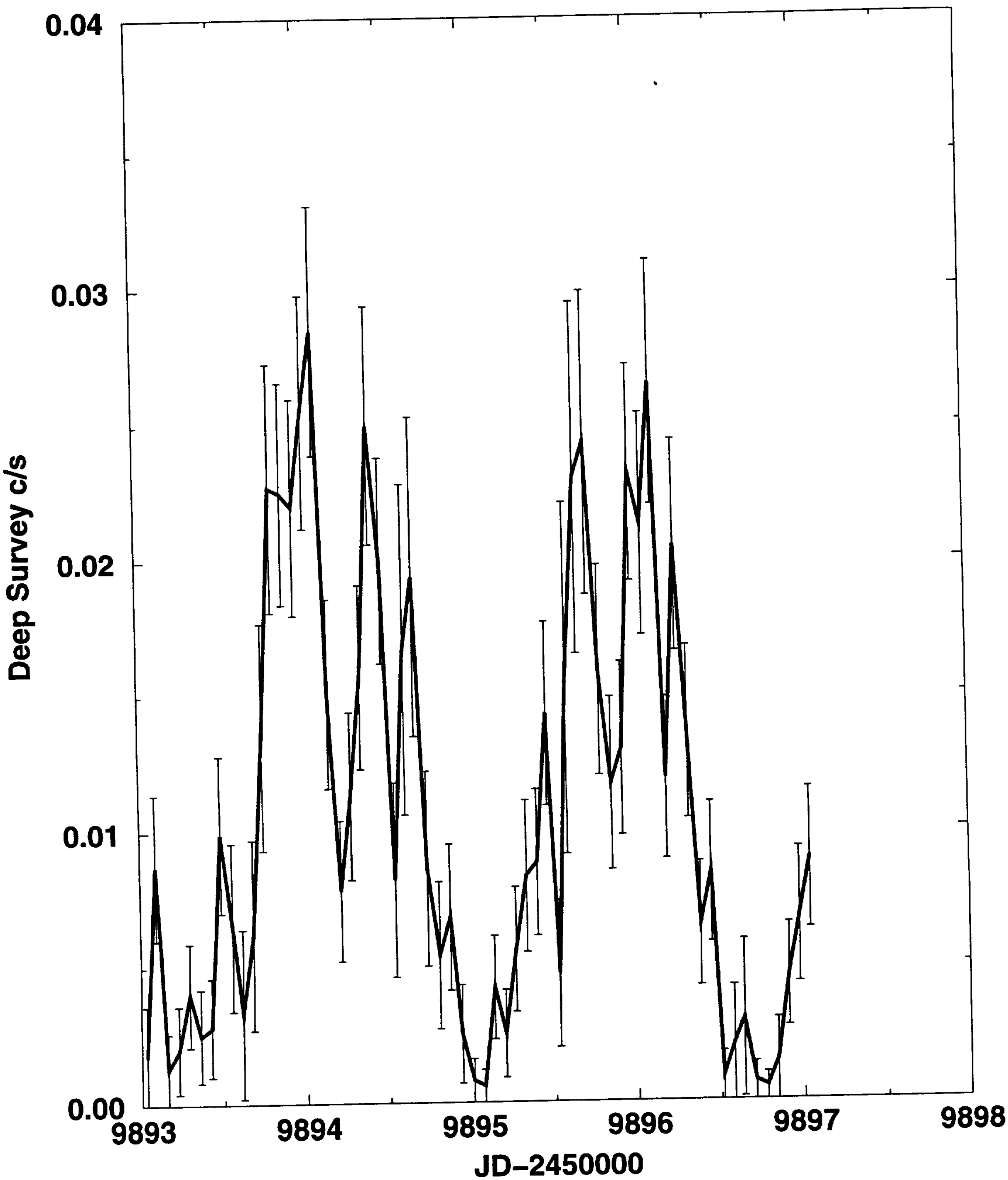
0.04
0.03
0.02
0.01
0.00
Deep Survey c/s
9893
9894
9895
9896
9897
9898
JD−2450000

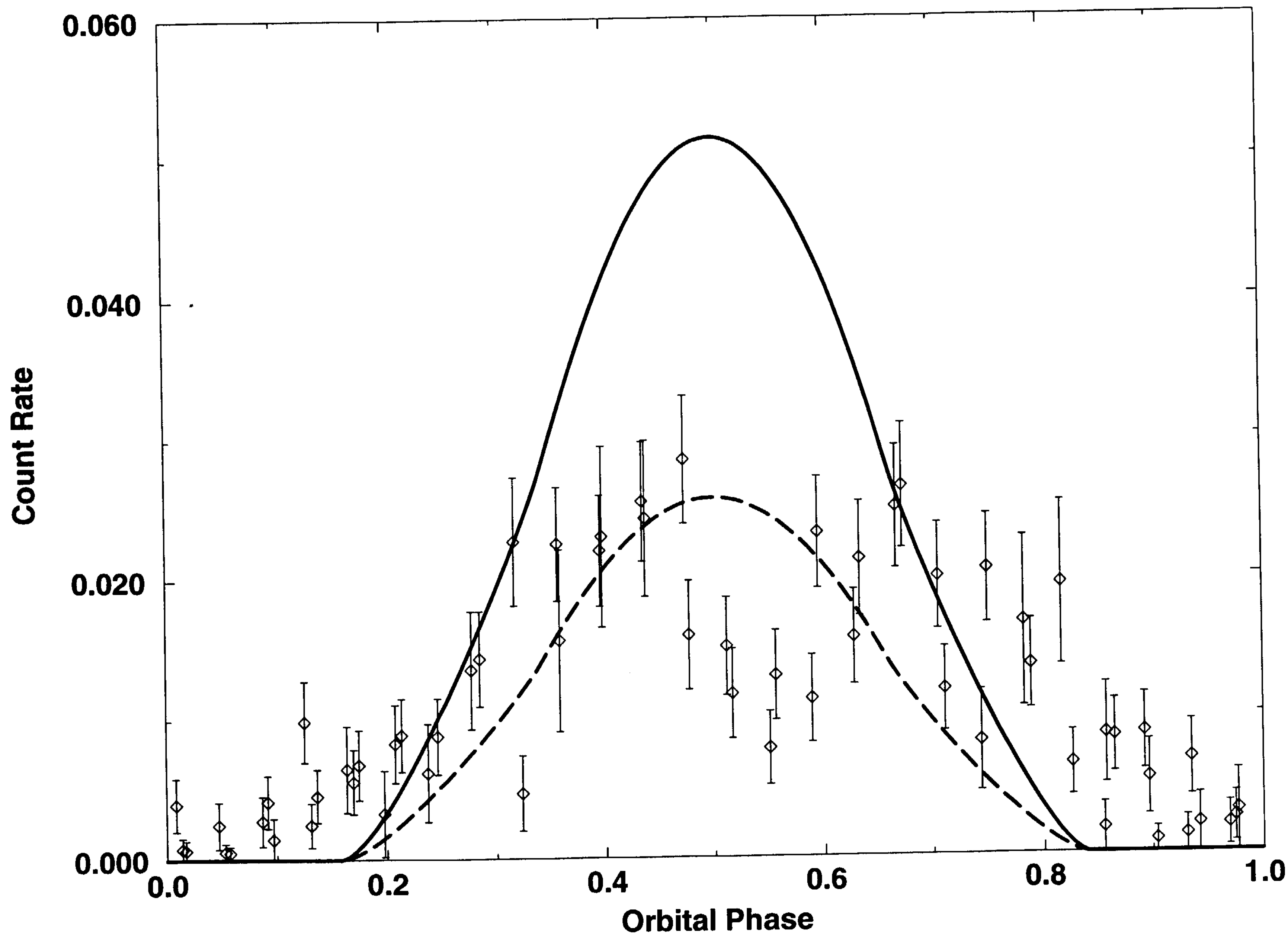

Count Rate
0.060
0.040
0.020
0.000
0.0
0.2
0.4
0.6
0.8
1.0
Orbital Phase

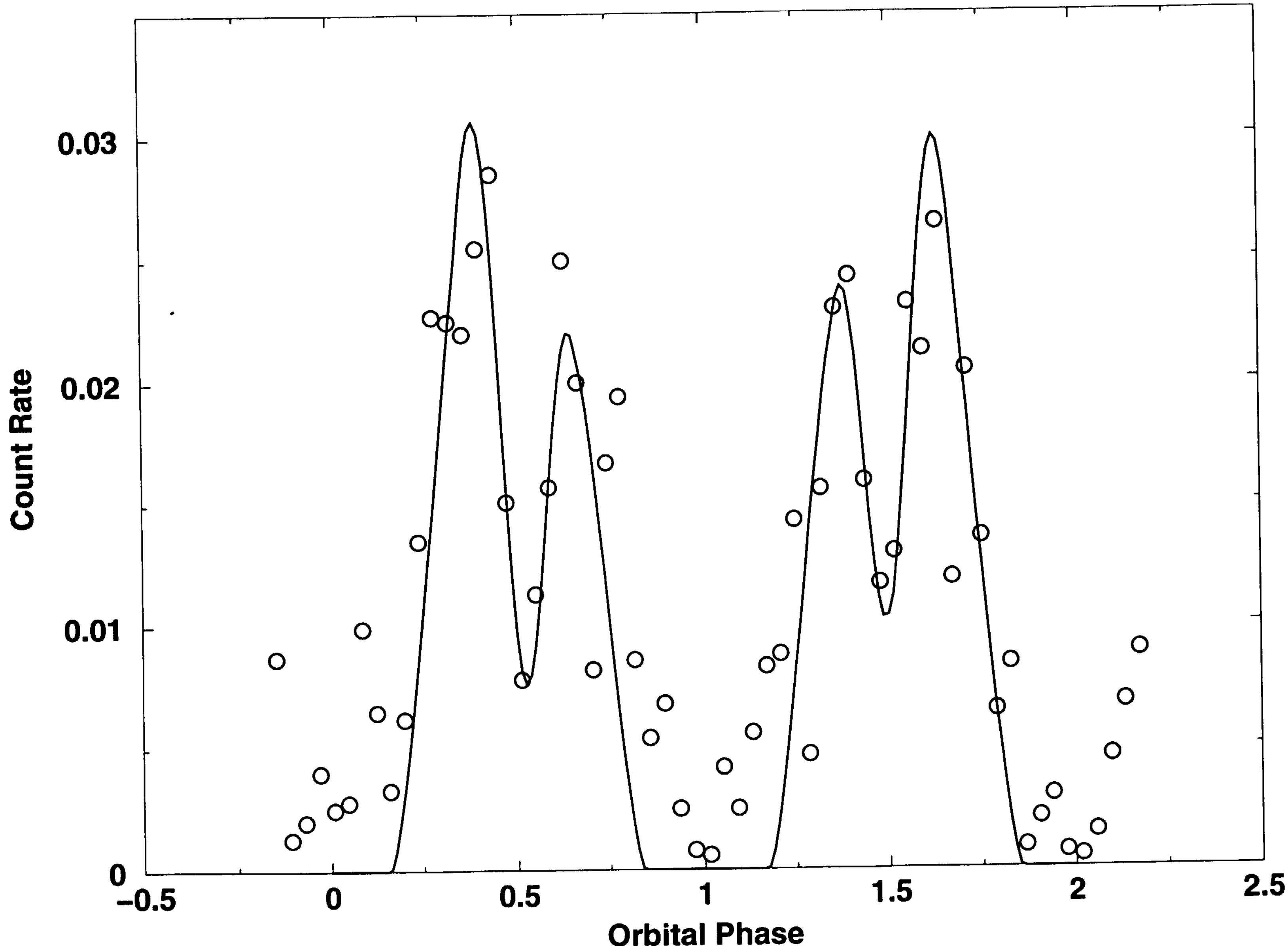
Count Rate
0.03
0.02
0.01
0
−0.5
0
0.5
1
1.5
2
2.5
Orbital Phase

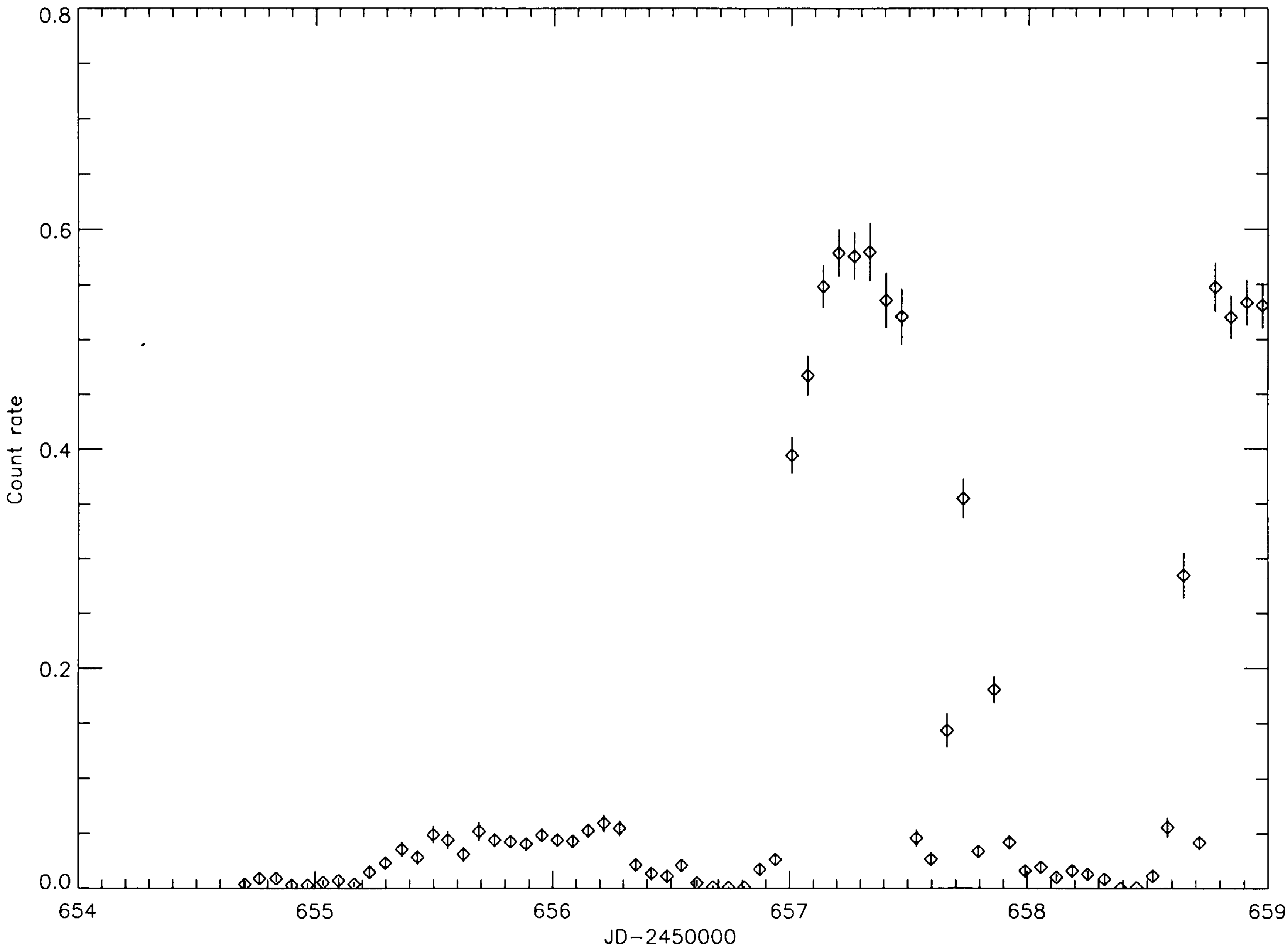
Count rate
0.0
0.2
0.4
0.6
0.8
654
655
656
657
658
659
JD-2450000

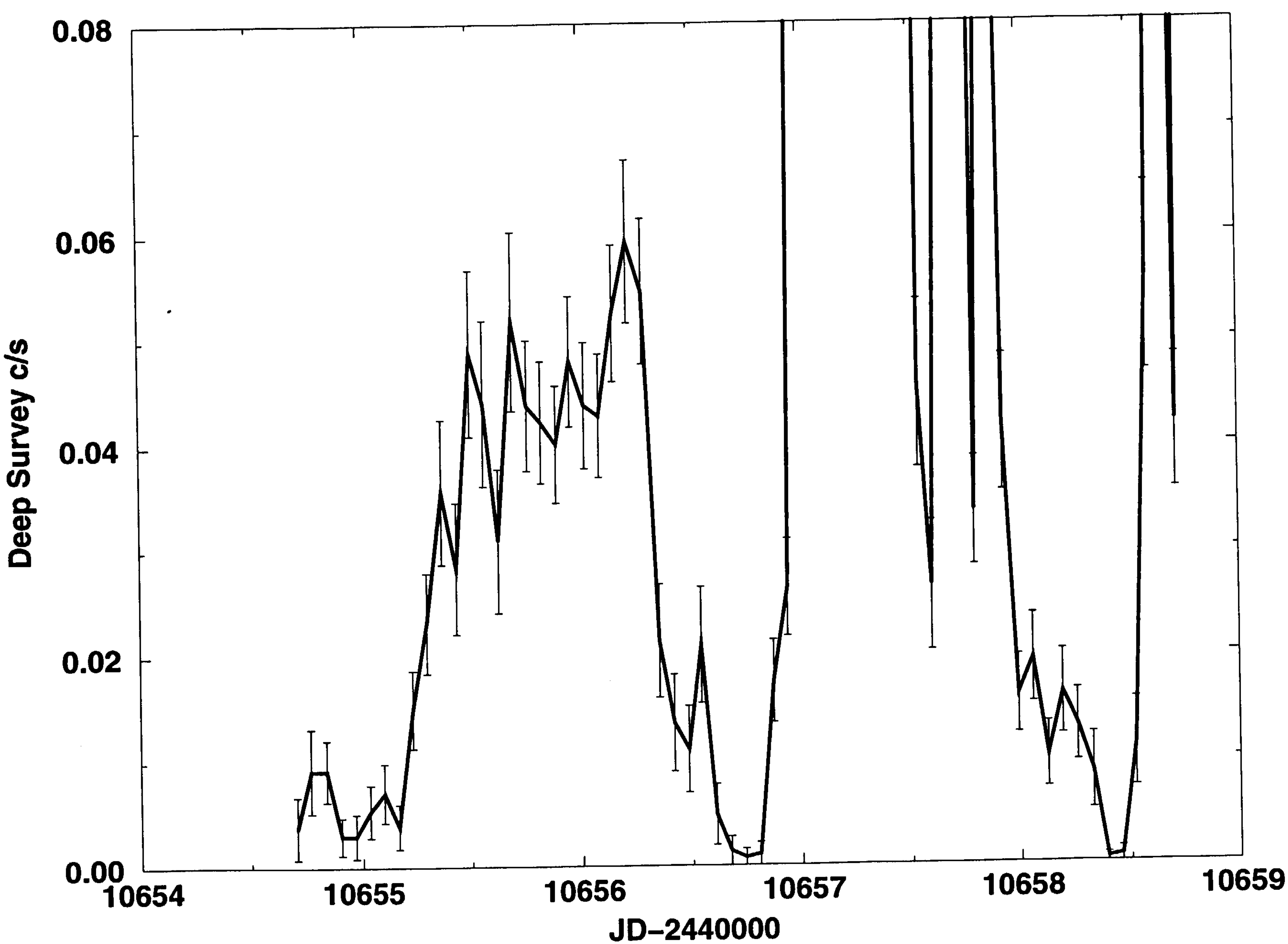
Deep Survey c/s
0.00
0.02
0.04
0.06
0.08
10654
10655
10656
10657
10658
10659
JD–2440000

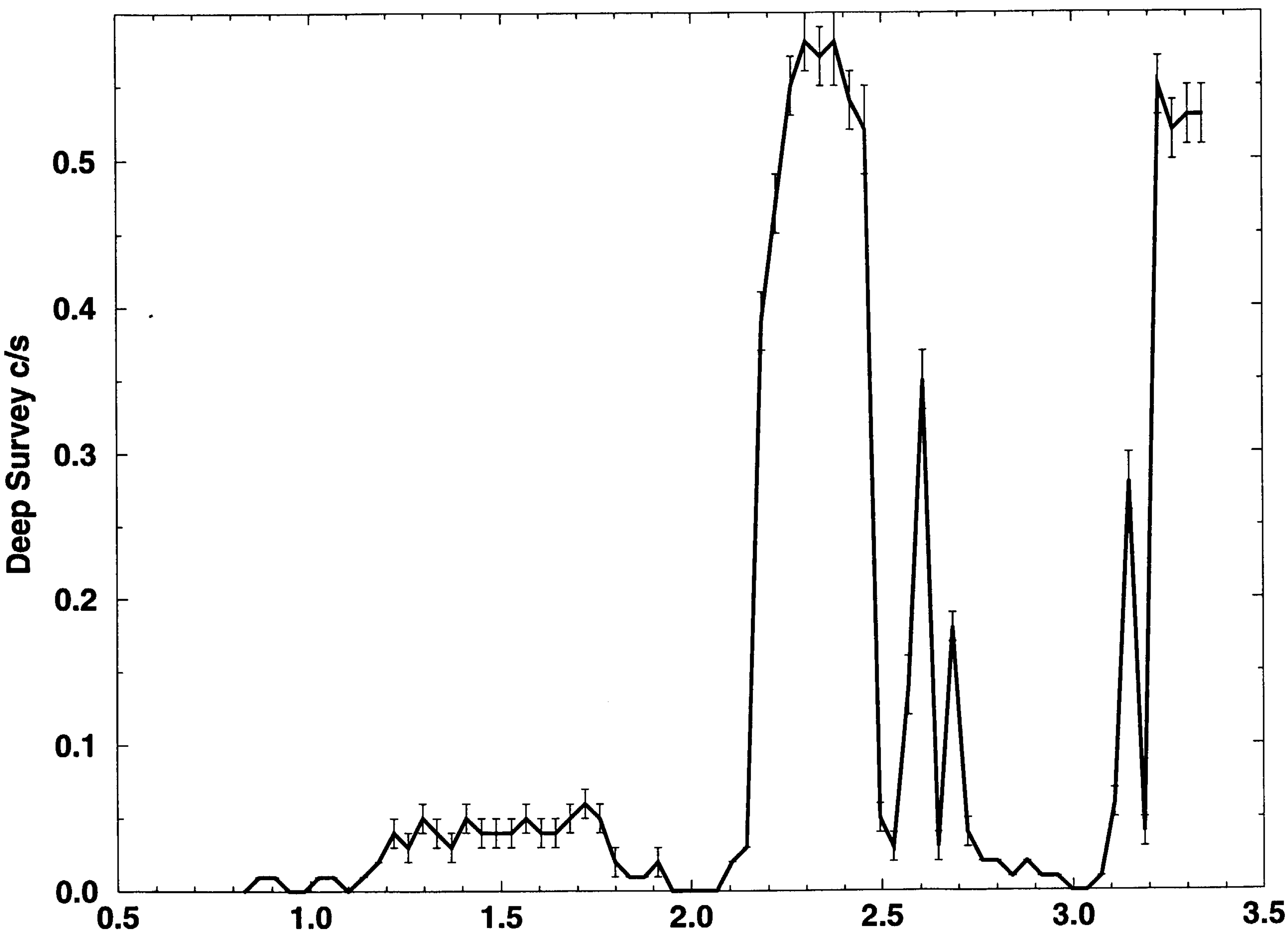
Deep Survey c/s
0.0
0.1
0.2
0.3
0.4
0.5
0.5
1.0
1.5
2.0
2.5
3.0
3.5

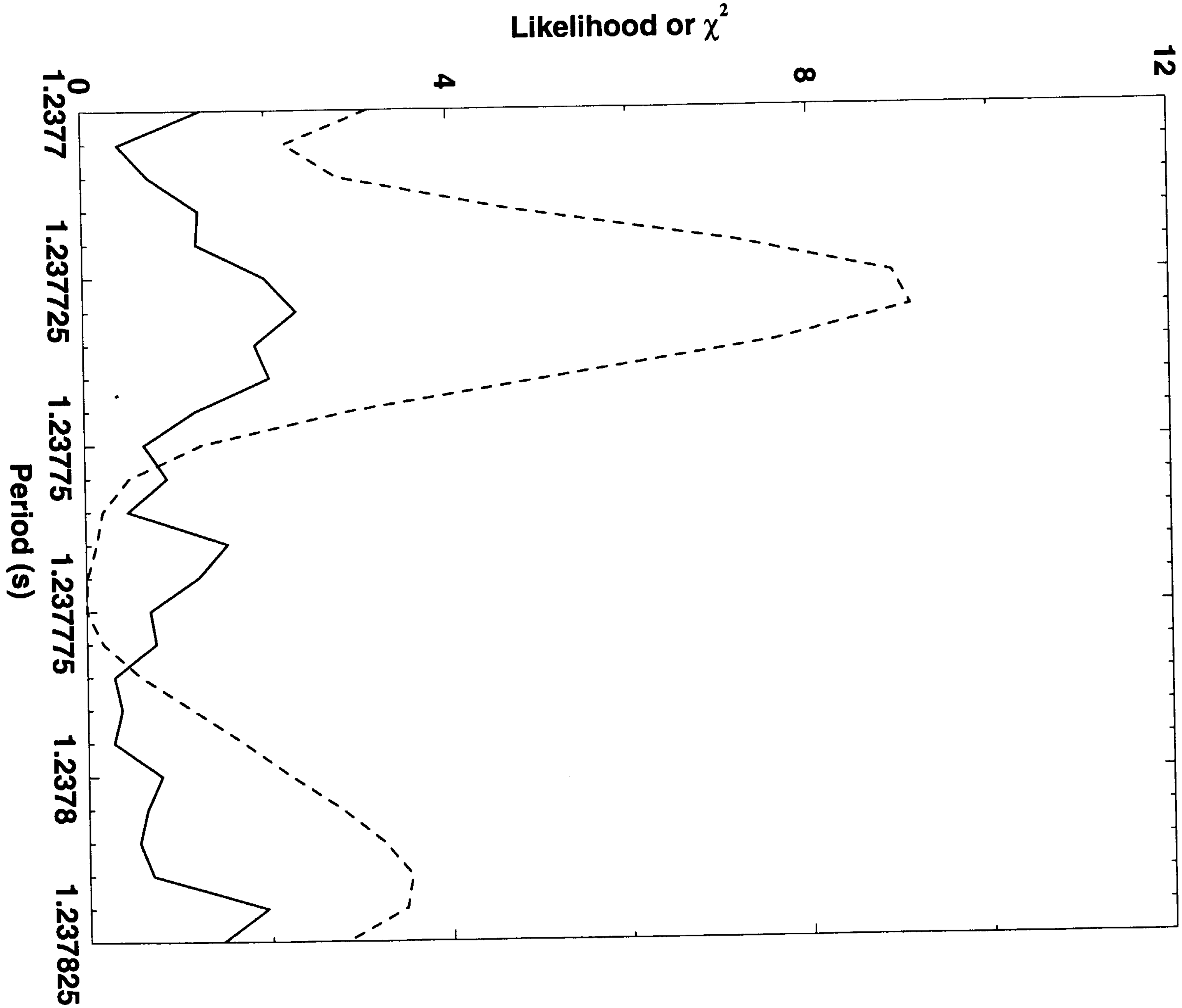
Likelihood or χ^2
0
4
8
12
1.2377
1.237725
1.23775
1.237775
1.2378
1.237825
Period (s)

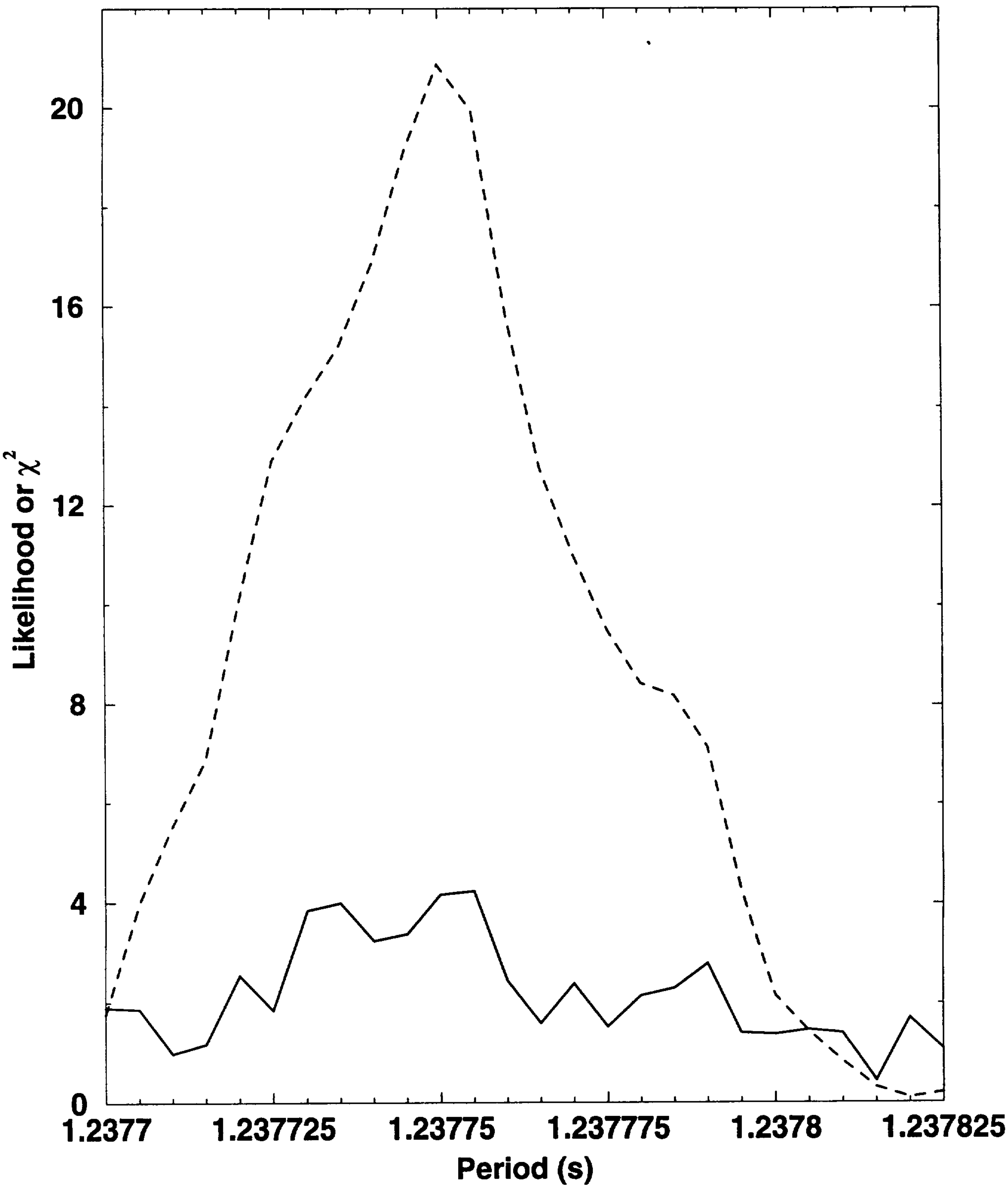

Likelihood or χ^2
0
4
8
12
16
20
1.2377
1.237725
1.23775
1.237775
1.2378
1.237825
Period (s)

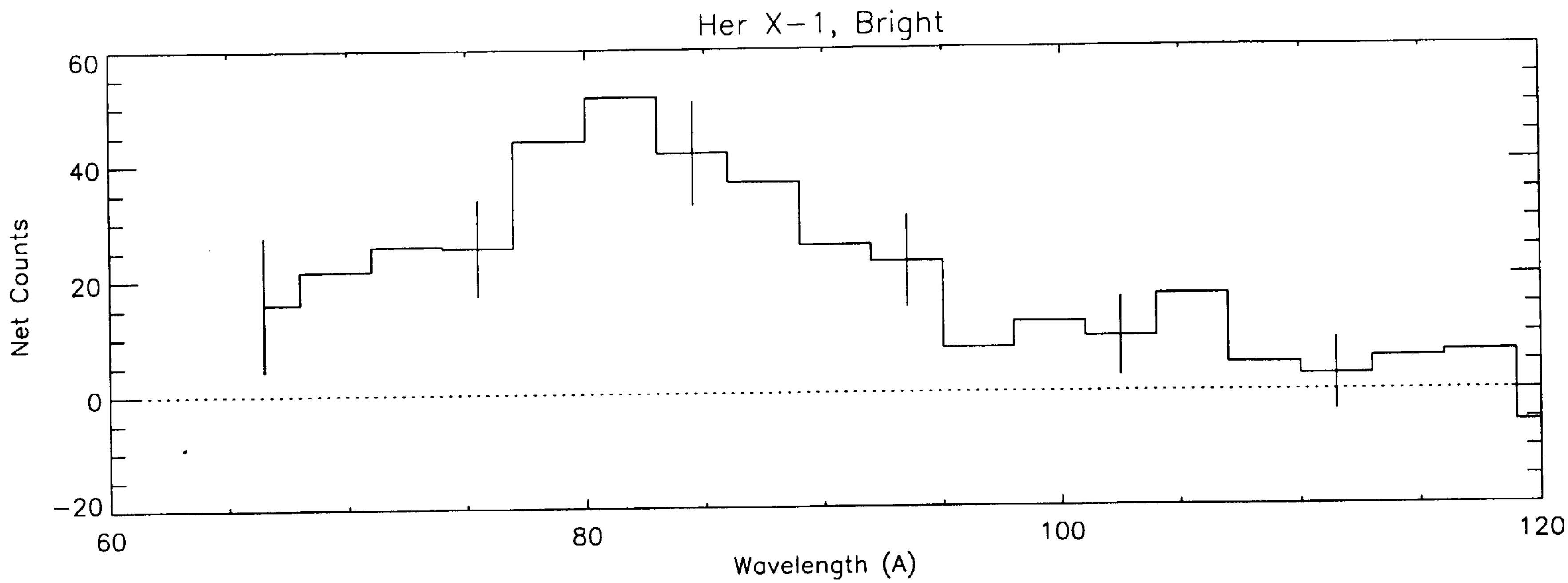
Her X−1, Bright
Net Counts
60
40
20
0
−20
60
80
100
120
Wavelength (A)

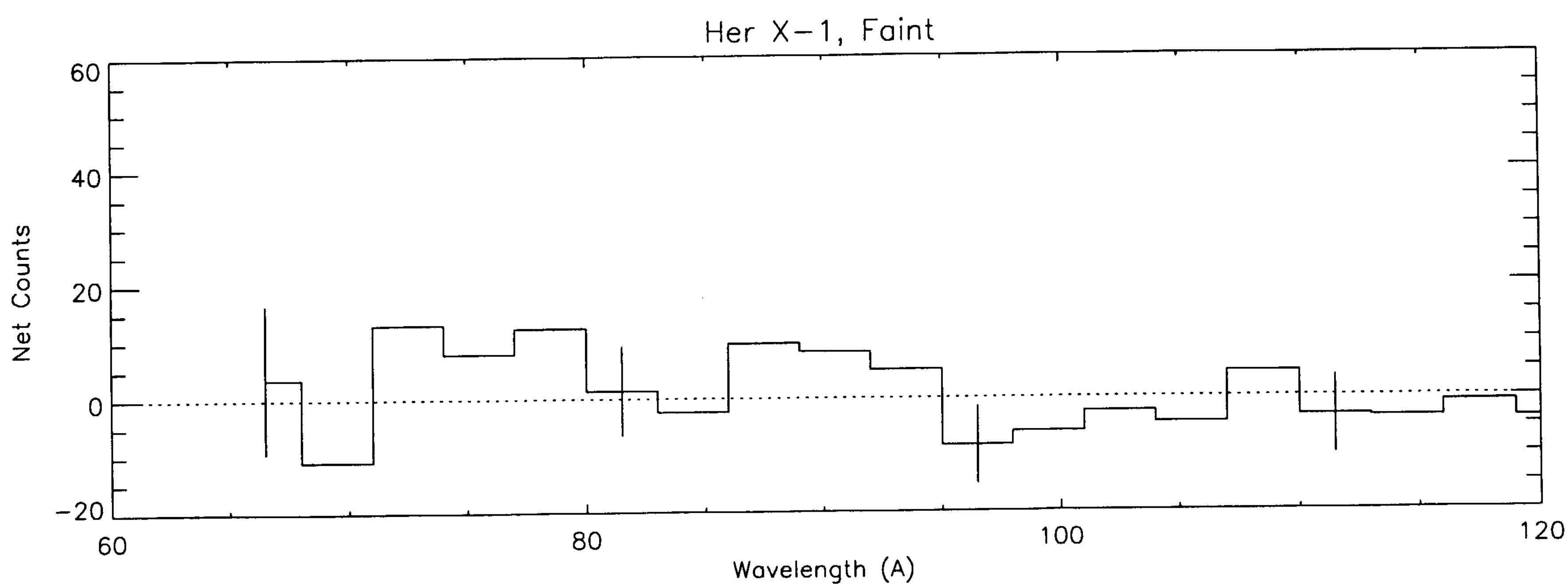
Her X−1, Faint
Net Counts
60
40
20
0
−20
60
80
100
120
Wavelength (A)

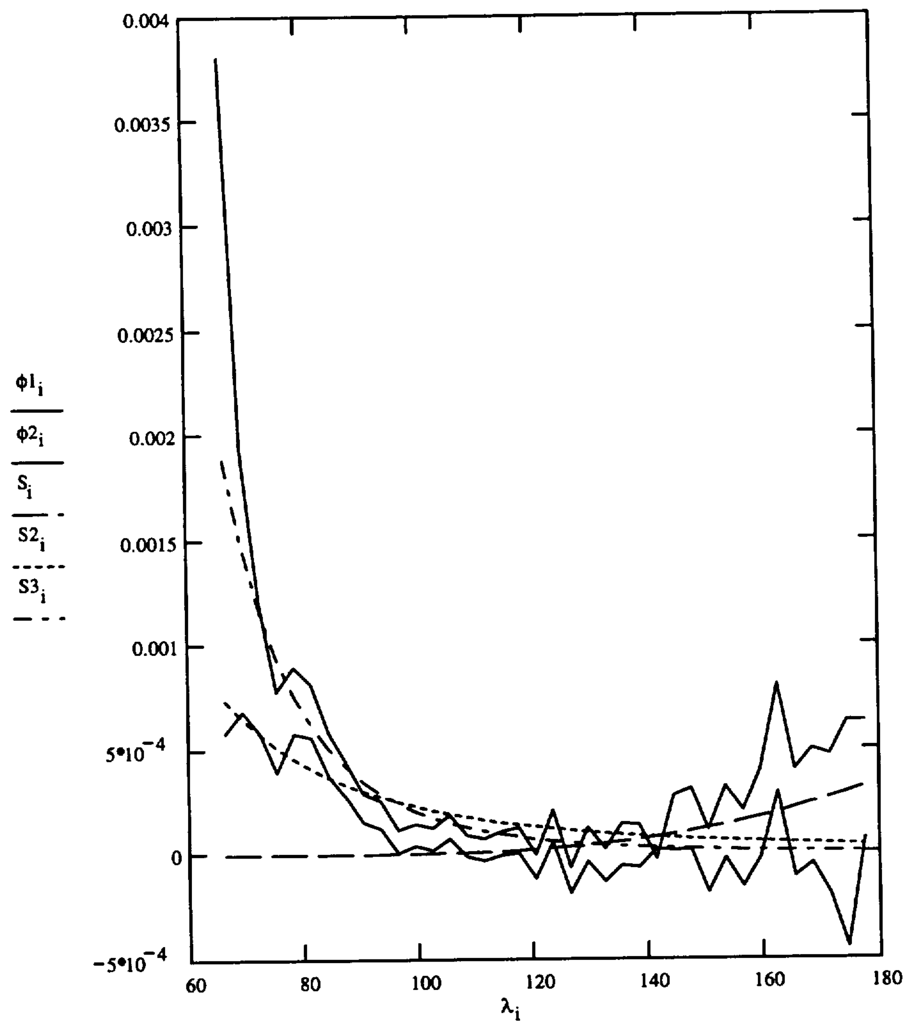

0.004
0.0035
0.003
0.0025
0.002
0.0015
0.001
5•10^-4
0
-5•10^-4
60
80
100
120
140
160
180
λi
φ1i
φ2i
Si
S2i
S3i

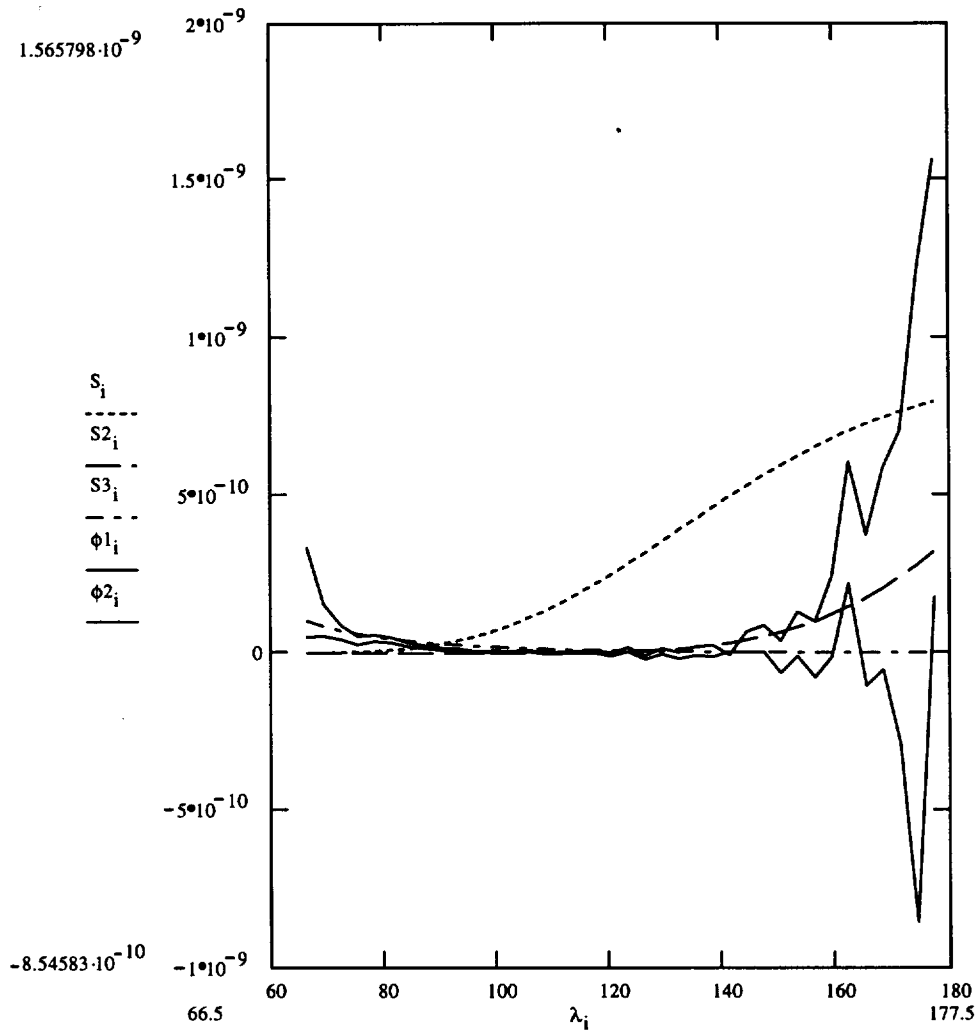
1.565798·10^-9
2•10^-9
1.5•10^-9
1•10^-9
5•10^-10
0
-5•10^-10
-8.54583·10^-10
-1•10^-9
S_i
S2_i
S3_i
ϕ1_i
ϕ2_i
60
80
100
120
140
160
180
66.5
λ_i
177.5

REPORT DOCUMENTATION PAGE

Form Approved
OMB No. 0704-0188

1. AGENCY USE ONLY (*Leave blank*)	2. REPORT DATE	3. REPORT TYPE AND DATES COVERED
	6/1/99	Final 5/13/98-5/12/99

4. TITLE AND SUBTITLE
The Origin of the EUV Emission in Her X-1

5. FUNDING NUMBERS
C S-92511-Z

6. AUTHOR(S)
D. A. Leahy and H. Marshall (P.I.)

7. PERFORMING ORGANIZATION NAME(S) AND ADDRESS(ES)
Eureka Scientific Inc.
2452 Delmer St., Ste. 100
Oakland, CA 94602

8. PERFORMING ORGANIZATION REPORT NUMBER

9. SPONSORING/MONITORING AGENCY NAME(S) AND ADDRESS(ES)

10. SPONSORING/MONITORING AGENCY REPORT NUMBER

11. SUPPLEMENTARY NOTES

12a. DISTRIBUTION/AVAILABILITY STATEMENT

12b. DISTRIBUTION CODE

13. ABSTRACT (*Maximum 200 words*)

Her X-1 exhibits a strong orbital modulation of its EUV Flux with a large decrease around time of eclipse of the neutron star, and a significant dip which appears at different orbital phases at different 35-day phases. We consider observations of Her X-1 in the EUVE by the Extreme Ultraviolet Explorer (EUVE), which includes data from 1995 near the end of the Short High state, and date from 1997 at the start of the Short High state. The observed EUV lightcurve has bright and faint phases. The ight phase can be explained as the low energy tail of the soft x-ray pulse. The faint phase emission has been modeled to understand its origin. We find: the x-ray heated surface of HZ Her is too cool to produce enough emission; the accretion disk does not explain the orbital modulation; however, reflection of x-rays off of HZ Her can produce the observed light curve with orbital eclipses.

14. SUBJECT TERMS	15. NUMBER OF PAGES
	16. PRICE CODE

17. SECURITY CLASSIFICATION OF REPORT	18. SECURITY CLASSIFICATION OF THIS PAGE	19. SECURITY CLASSIFICATION OF ABSTRACT	20. LIMITATION OF ABSTRACT

NSN 7540-01-280-5500

Standard Form 298 (Rev. 2-89)
Prescribed by ANSI Std Z39-18
298-102